Hindawi
Security and Communication Networks
Volume 2017, Article ID 2524513, 12 pages
https://doi.org/10.1155/2017/2524513

Research Article

Design and Analysis of Self-Healing Tree-Based Hybrid Spectral Amplitude Coding OCDMA System

Waqas A. Imtiaz,[1] Affaq Qamar,[1] Atiq Ur Rehman,[2] Haider Ali,[1] Adnan Rashid Chaudhry,[2] and Javed Iqbal[3]

[1]*Department of Electrical Engineering, Abasyn University, Peshawar, Pakistan*
[2]*Faculty of Computing and Information Technology, Northern Border University, Rafha, Saudi Arabia*
[3]*Sarhad University of Science and Information Technology, Peshawar, Pakistan*

Correspondence should be addressed to Waqas A. Imtiaz; waqasahmed15@gmail.com

Received 6 February 2017; Accepted 15 May 2017; Published 20 June 2017

Academic Editor: Vincenzo Conti

This paper presents an efficient tree-based hybrid spectral amplitude coding optical code division multiple access (SAC-OCDMA) system that is able to provide high capacity transmission along with fault detection and restoration throughout the passive optical network (PON). Enhanced multidiagonal (EMD) code is adapted to elevate system's performance, which negates multiple access interference and associated phase induced intensity noise through efficient two-matrix structure. Moreover, system connection availability is enhanced through an efficient protection architecture with tree and star-ring topology at the feeder and distribution level, respectively. The proposed hybrid architecture aims to provide seamless transmission of information at minimum cost. Mathematical model based on Gaussian approximation is developed to analyze performance of the proposed setup, followed by simulation analysis for validation. It is observed that the proposed system supports 64 subscribers, operating at the data rates of 2.5 Gbps and above. Moreover, survivability and cost analysis in comparison with existing schemes show that the proposed tree-based hybrid SAC-OCDMA system provides the required redundancy at minimum cost of infrastructure and operation.

1. Introduction

Adaptation of passive optical network (PON) requires an efficient multiple access technology that can support maximum number of subscribers at high data rates and extended reach. Time division multiplexed (TDM) PON is deployed to provide the necessary broadband services in access domain. However, the time-sharing property of TDM PON limits the amount of data per subscriber. Consequently, wavelength division multiplexed (WDM) technology is adapted to enhance network capacity in terms of data and the number of subscribers. Nevertheless, deployment of WDM-PON is limited by the use of relatively expensive components at both the transmitter and receiver modules. Moreover, the scarcity of available wavelengths confines the use of WDM-PON for large number of subscribers in next-generation PONs [1]. Consequently, optical code division multiple access (OCDMA) systems are expected to solve the last-mile bottleneck between high speed core/metro networks and access domain [1–4].

Among all OCDMA systems for the access domain, spectral amplitude coding (SAC) family has gained significant attention because of the desirable correlation properties, flexibility of implementation, and support for high transmission capacity [5]. SAC-OCDMA coding schemes are a family of K binary $[0's\ 1's]$ sequences characterized by auto- and cross-correlation (λ_c) properties along with desirable length (N) and weight (w) [4–6]. An optimal SAC-OCDMA coding scheme is one that provides desirable BER, $\leq 10^{-9}$, by reducing multiaccess interference (MAI) and associated phase induced intensity noise (PIIN) through suitable correlation properties, minimum length, large weights, flexibility of implementation, and reduced hardware complexity. Several coding algorithms have been designed in SAC family to provide high capacity along with extended reach; however,

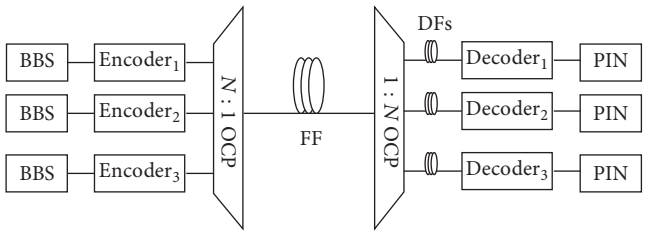

Figure 1: Conventional SAC-OCDMA system.

the use of suitable binary sequence is still an open issue [3, 5, 7–10].

Another problem that limits the deployment of SAC-OCDMA system at access domain is the lack of a suitable protection mechanism [13, 14]. Conventional SAC-OCDMA systems are built with tree architecture that utilize a long feeder fiber (FF) to connect optical line terminal (OLT), at CO, with remote node (RN) at the subscriber premises as shown in Figure 1. End-face of the passive RN connects multiple optical network units (ONUs) through short span dedicated distribution fibers (DFs). Figure 1 shows the basic architecture of SAC-OCDMA system, where no protection is provided between CO and ONUs [3, 4]. This significantly elevates the loss of data in case of failures at optical components (including fibers). Therefore, it is imperative to design an efficient protection mechanism that facilitates the detection and recovery of cuts/failures throughout the network, in order to ensure the success of SAC-OCDMA technology at the access domain.

This paper proposes an efficient SAC-OCDMA system with high transmission capacity, through enhanced multidiagonal (EMD) code. Moreover, a robust tree-based hybrid protection architecture is proposed for survivability enhancement along with self-healing capacity at both feeder and distribution fibers. The proposed solution includes a new star-ring protection architecture that provides preplanned redundancy without duplicating the entire fiber setup at distribution network. Performance of the proposed tree-based hybrid system is analyzed using comprehensive analytical and simulation analysis by referring to bit error rate (BER) and eye patterns. Redundancy operation of the proposed system is also observed for failures at both feeder and distribution fibers. Furthermore, capital expenditure (CAPEX) and operation expenditure (OPEX) of the proposed setup are also computed to determine the feasibility of implementation in comparison with existing solutions.

Rest of the paper is organized as follows. Section 2 discusses the construction of EMD code followed by a detailed design and implementation of the proposed architecture in Section 3. Analytic and simulation analysis for transmission capacity of the proposed setup is performed in Section 4. Section 5 covers the survivability analysis of the proposed tree-based SAC-OCDMA system for failures at the feeder and distribution levels. Detailed cost analysis is presented in Section 6 that is followed by the final conclusion in Section 7.

2. Enhanced Multidiagonal Code

EMD code is used in the proposed system to achieve the required transmission capacity in terms of data, reach, and number of subscribers. EMD code is designed with two-matrix structure including data matrix (D_n) and code matrix (C_n). Chips in D_n are used to encode the data bits after spectral translation, whereas C_n chips refer to the code bits that are embedded to elevate the performance of EMD based SAC-OCDMA system [15]. Moreover, EMD coding algorithm is designed with three basic performance parameters including N, w, and λ_c between adjacent codes. The following section outlines the properties of D_n and C_n, followed by the implementation of EMD matrix.

$$\text{EMD} = \left[D_n \mid C_c\right]_{K\times N}. \tag{1}$$

2.1. Data Matrix. D_n consists of a $K \times K$ diagonal matrix, where K rows and K columns of the matrix represent number of subscribers and length of D_n, respectively. Furthermore, D_n is designed with multiple rows of length K, $w = 1$, and $_c = 0$. Therefore, the basic 2×2 D_n can be written as

$$D_n = \begin{bmatrix} 1 & 0 \\ 0 & 1 \end{bmatrix}. \tag{2}$$

2.2. Code Matrix. C_n consists of a $K \times J$ matrix, where K rows and J columns represent the number of subscribers and length of the matrix, respectively. C_n for EMD code is designed with multiple rows of $J = K + 1$, $w = 2$, and $_c = 1$ between the codes in adjacent rows. The basic 2×3 C_n can be written as

$$C_n = \begin{bmatrix} 0 & 1 & 1 \\ 1 & 1 & 0 \end{bmatrix}. \tag{3}$$

Consequently, the proposed EMD code while using (1) and the properties of D_n, C_n is given by

$$\text{EMD}_2 = \left[\begin{array}{cc|ccc} 1 & 0 & 0 & 1 & 1 \\ 0 & 1 & 1 & 1 & 0 \end{array}\right]_{2\times 5}. \tag{4}$$

Equation (4) shows that $'1, 2, 1'$ combination is maintained between adjacent EMD codes. The number of subscribers in EMD code can be increased through simple diagonal mapping, while maintaining the respective properties of D_n and C_n. This increases the cardinality of SAC-OCDMA system with minimum impact on N for EMD code. Consequently, EMD code matrix for 4 subscribers is given by

$$\text{EMD}_4 = \left[\begin{array}{cccc|ccccc} 1 & 0 & 0 & 0 & 0 & 0 & 0 & 1 & 1 \\ 0 & 1 & 0 & 0 & 0 & 0 & 1 & 1 & 0 \\ 0 & 0 & 1 & 0 & 0 & 1 & 1 & 0 & 0 \\ 0 & 0 & 0 & 1 & 1 & 1 & 0 & 0 & 0 \end{array}\right]_{4\times 9}. \tag{5}$$

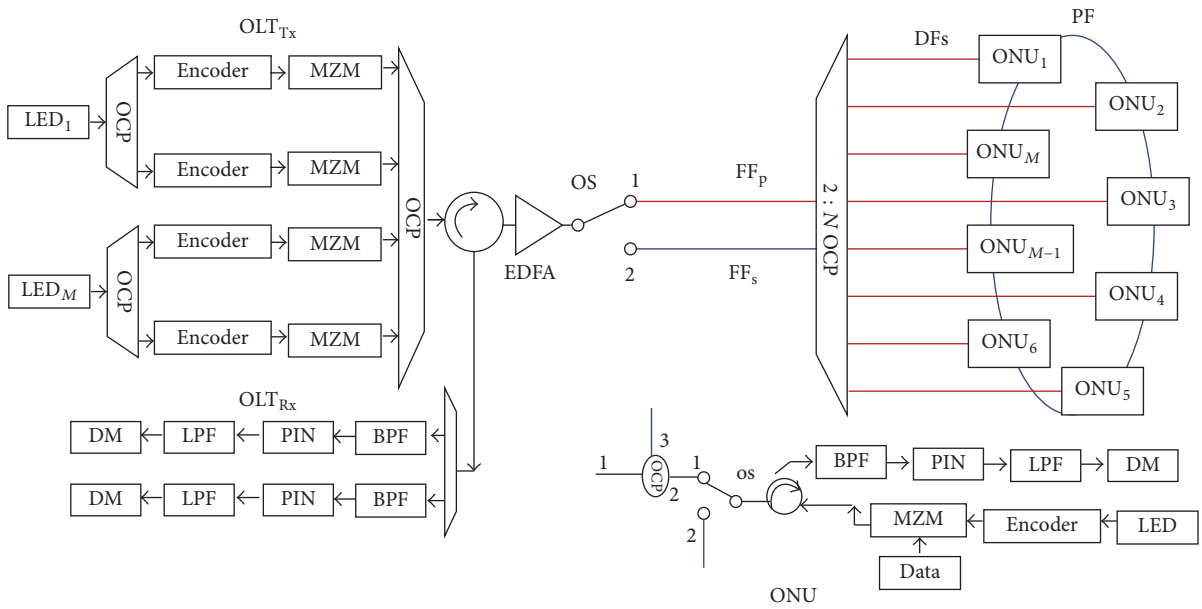

Figure 2: Proposed tree-based hybrid SAC-OCDMA system.

2.3. Properties of EMD Code

(i) EMD code can be designed with $w \geq 3$.

(ii) Length N of each code is equal to $K + [K(K-2)+1]$.

(iii) $\lambda_c = 1$ between adjacent codes, only, of the EMD matrix.

(iv) Auto- and cross-correlation properties of EMD code, when $B_k(i)$ denotes the ith element of Kth EMD code, are given by

$$\sum_{i=1}^{N} B_k(i)\, B_l(i) = \begin{cases} w; & k = l \\ 1; & k \neq l \text{ for adjacent code} \\ 0; & k \neq l \text{ otherwise.} \end{cases} \quad (6)$$

3. Proposed SAC-OCDMA System

The proposed tree-based hybrid SAC-OCDMA system consists of the following components.

3.1. Central Office. Central office is located at the service provider premises and houses multiple OLT ports, which generates required services towards the PON distribution network. OLT consists of the following.

3.1.1. Optical Source. Optical source is crucial in designing an efficient and reliable SAC-OCDMA system because of its significant effect on the cost and performance of PON [3, 16]. OCDMA systems can be classified into two types, according to the choice of optical sources: coherent and in-coherent OCDMA. Prior system requires highly coherent, ultra-short light pulses (MLL, supercontinuum laser, etc.) in order to maintain nominal BER in high capacity systems. Such sources are difficult to tune and involve precise laser positioning to assure efficient performance. This significantly increases the cost and complexity of the OCDMA system.

Moreover, localized power distribution in coherent optical sources requires complex equipment to translate binary $0's$ and $1's$ into spectral representation. Most of the encoders require complex tuning and fast electronic circuits that further elevates the cost and complexity of implementation for coherent SAC-OCDMA systems at the last-mile section of the network [17].

Broadband sources (BBSs) with relatively same power distribution throughout their bandwidth facilitate the required encoding at the expense of simple setup. Moreover, BBSs like light emitting diodes (LEDs) have shown efficient performance with simple in-coherent decoding techniques including balanced and direct detection [16]. Furthermore, SAC-OCDMA systems are targeted to support economical access networks; therefore, optical source with low cost, simple drive circuits, flexibility of encoding, immunity to beat noise, and stable performance are suitable for implementation of the proposed tree-based hybrid SAC-OCDMA system for PON.

Thus, OLT for the proposed system contains an array of LEDs, which are tuned at different wavelengths to support desirable number of subscribers. Output from the LED is fed into 1 : 3 optical coupler (OCP) in order to provide the required spectrum for code chips at input of the encoder as shown in Figure 2.

3.1.2. Encoder. Design of a suitable encoder is observed, as of critical concern for the implementation of SAC-OCDMA system in terms of functioning and ability to perform the required encoding. Various devices have been proposed for encoding operation in SAC-OCDMA system; however, the use of suitable device is still an open issue [3, 4, 18, 19].

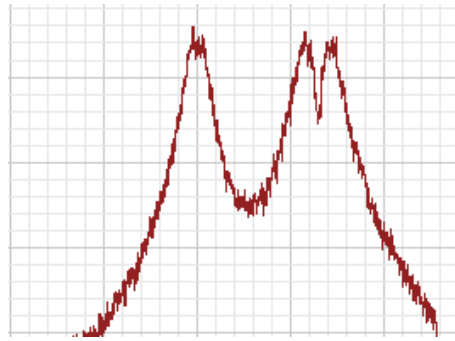

Figure 3: Spectral representation of encoded [0 0 1 0 1 1 0 0 0] bits in EMD code.

This paper utilizes optical multiplexer (MUX) for translating the proposed binary sequence into spectral representation at OLT [7, 8]. Each input of the optical MUX contains a bandpass filter, which is tuned to select the desired spectrum in accordance with EMD chips. Figure 3 represents the implementation of EMD code [0 0 1 0 1 1 0 0 0] through a 3:1 MUX, with 0.4 nm bandpass Bessel filters at the input. It is observed that the proposed arrangement can efficiently perform the required binary to optical conversion with maximum precision and simple architecture.

End-face of the optical encoder is connected with Mach-Zehnder Modulator (MZM), which combines optical signal with data from individual subscriber. Output of the modulating arrangement is applied to $N:1$ OCP with N input and 1 output port as shown in Figure 2. OCP is further connected with a three-port optical circulator (OC_{co}) that is fed into switching arrangement (SA) through an erbium doped fiber amplifier (EDFA).

3.1.3. Switching Arrangement. Switching arrangement (SA_{co}) consists of a 1:2 optical switch (OS_{sa}) that connects OLT with both primary and secondary feeder fibers (FF_p, FF_s) as shown in Figure 2. OS_{sa} is used to perform the necessary switching between FF_p and FF_s, when a cut/failure occurs at the feeder fiber. Under normal mode of operation, OS_{sa} is at position 1, and all traffic is supplied through FF_p. Position of the proposed OS_{sa} is controlled by OLT medium access control (MAC) layer, which is responsible for fault detection and restoration at the feeder level. Consequently, no extra arrangement is required for changing OS_{sa} positions for seamless transmission between OLT and ONU modules.

3.2. Remote Nodes. The proposed tree-based hybrid SAC-OCDMA system utilizes a single remote node to facilitate communication between CO and subscriber premises. RN houses a $2:N$ OCP that connects each ONU with both FF_p and FF_s at the input and short span dedicated DFs at the end-face as shown in Figure 2. RN facilitates ubiquitous transmission of down- and upstream traffic by simultaneously connecting each ONU with both FF_p, FF_s fibers. This allows the proposed system to immediately restore the flow of affected traffic in case of failure across the network.

3.3. Optical Network Unit. Optical network unit $\{ONU_m; m = 1, 2, 3, \ldots, M\}$ consists of a 1:2 OCP with 3 ports as shown in Figure 2. Ports 1 and 2 are connected to dedicated DF_m and a 2:1 optical switch OS_{onu_m}, respectively. Port 3 extends the ring based protection fiber (PF_r) towards its neighboring ONUs. Ring based redundancy arrangement provides the required preplanned protection without duplicating entire fiber at the distribution network. Moreover, use of star-ring topology eliminates the significant power loss that is encountered in single-ring based PON [13, 20–22].

OS_{onu_m} is at position 1, under normal mode of operation, and all traffic is being sent and received though dedicated DFs. While in case of failure at the DF, optical switch is moved towards position 2, which connects the effected ONU with redundant PF_r. Fault detection and switching operation at distribution level are controlled through ONU_m MAC layer in order to avoid extra arrangement for network survivability at ONU modules.

End-face of OS_{onu_m} is fed into a three-port optical circulator (OC_{onu}), which is further connected with ONU_m receiving module as shown in Figure 2. ONU receiver module consists of a bandpass filter (for SDD technique), which recovers the nonoverlapping spectral chip, D_n, only. Output of decoding arrangement is connected with PIN photodiode, which is fed into Bessel low pass filter (LPF) followed by decision-making (DM) circuit.

3.3.1. Spectral Direct Detection Technique. SDD technique is readily employed for coding schemes with ideal cross-correlation properties, owing to its significant advantages like simple implementation, minimum expenditure, and removal of MAI and associated PIIN at the receiving photodiode. The principle of SDD technique is based on the recovery of nonoverlapping spectral chip only, rendering maximum autocorrelation with the intended signal and minimum cross-correlation with interferer's [7, 23].

This technique is implemented through a simple bandpass filter, which is centered to recover the nonoverlapping spectral chip only. However, it is necessary to send the entire coded spectrum, in order to maintain integrity of the full address along with efficient power at the receiving photodiode. Figure 4 shows the implementation of SDD technique at the receiving ONU in the proposed setup. Decoding arrangement consists of a single bandpass filter, which is centered to recover D_n chip only. This operation

Table 1: Description and specification of noise variance parameters in (8).

Description	Parameters	Values
Electron charge	e	1.602×10^{-19}
Receiver noise equivalent electrical bandwidth	B	500 MHz
Boltzmann's constant	K_b	1.38×10^{-23}
Receiver noise absolute temperature	T_n	300 K
Receiver load resistance	R_L	1030 Ω
Quantum efficiency	η	0.6
Plank's constant	h	6.6260×10^{-34}
Optical source bandwidth	Δv	3.75×10^{12}
Optical wavelength	λ	1550 nm
Effective power of BBS at the receiver	P_{sr}	−10 dBm

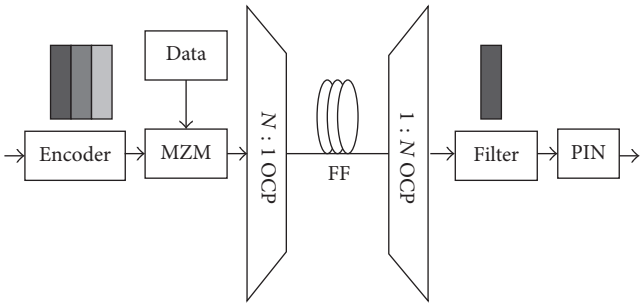

Figure 4: Spectral direct detection technique.

eradicates MAI and associated PIIN, since the overlapping spectrum at the transmitted C_n is removed before the signal is converted to electrical domain [4, 7].

4. Performance Analysis

Conversion of the received optical signal into electrical domain is accompanied with shot, PIIN, and thermal noises generated at the PIN photodiode. Presence of these noise sources significantly reduces quality of the received signal, which elevates BER at the receiving end. Therefore, it is imperative to determine performance of the proposed tree-based hybrid SAC-OCDMA system in the presence of shot, PIIN, and thermal noises at the receiving photodiode.

4.1. Analytic Analysis. Performance of the proposed tree-based hybrid SAC-OCDMA system is analyzed with reference to signal to noise ratio (SNR) and BER of EMD code at the encoder and SDD at the decoder. Gaussian approximation is used to evaluate the performance while considering noise powers at the receiving end [4]. If I represents the incident current, I^2 represents the power spectral density (PSD), and σ^2 gives noise variance at the receiving photodiode. Then the total SNR is given by [8, 15]

$$\text{SNR} = \left[\frac{I^2}{\sigma^2}\right], \tag{7}$$

where σ^2 is the sum of shot $\langle i^2_{\text{shot}}\rangle$, PIIN $\langle i^2_{\text{PIIN}}\rangle$, and thermal $\langle i^2_{\text{thermal}}\rangle$ noise powers, which can also be written as

$$\sigma^2 = 2eBI + I^2 B\tau_c + \frac{4K_b T_n B}{R_L}. \tag{8}$$

Table 1 shows the specifications and description of σ^2 parameters in (8). Moreover, the coherent time τ_c of intensity noise terms in the photodiode output is given by

$$\tau_c = \frac{\int_o^\infty G(v)^2\, dv}{\left[\int_o^\infty G(v)\, dv\right]^2}. \tag{9}$$

$G(v)$ in (9) shows the PSD at the receiving photodiode. In order to analyze performance of the proposed tree-based hybrid SAC-OCDMA system while using Gaussian approximation, it is assumed that each optical source is ideally polarized with smooth spectrum throughout its bandwidth. Moreover, PIN photodiodes receive identical spectral width and power (P_{sr}) from each optical source [4, 7, 8].

If $B_k(i)$ denotes the ith element of Kth EMD code, then the correlation properties at SDD based decoder, if the required information is recoverable from D_n chip only, are given by

$$\sum_{i=1}^{N} B_k(i)\, B_l(i) = \begin{cases} w, & \forall k = l \\ 0, & \forall k \neq l. \end{cases} \tag{10}$$

For the incident current,

$$I = \Re \int_o^\infty G(v)\, dv. \tag{11}$$

PSD under the effect of various noise sources is given by

$$G(v) = \frac{P_{sr}}{\Delta v} \sum_{k=1}^{K} d_k \sum_{i=1}^{N} B_k(i)\, B_l(i) \left[u\left(\frac{\Delta v}{N}\right)\right]. \tag{12}$$

P_{sr}, Δv, and u in (12) show the power at input of the PIN photodiode, line-width of LED, and unit step function,

respectively. For total I at the receiving photodiode, (12) is integrated from 0 to ∞

$$\int_0^{\infty} G(v)\,dv = \int_0^{\infty} \frac{P_{sr}}{\Delta v} \sum_{k=1}^{K} d_k \sum_{i=1}^{N} B_k(i)\, B_l(i) \left\{ u\left[\frac{\Delta v}{N} \right] \right\} dv. \tag{13}$$

$\sum_{k=1}^{K} d_k$ in (13) represent the transmitted bit, either 0 or 1, by a single subscriber. Equation (13) can be simplified by using the correlation properties in (10), which leads to

$$\int_0^{\infty} G(v)\,dv = \frac{P_{sr} w}{N}. \tag{14}$$

Now the total incident current from (14) can be written as

$$I = \Re \frac{P_{sr} w}{N}. \tag{15}$$

$\Re$ represents responsitivity of the receiving photodiode, given by $\Re = \eta e / h v_c$. Table 1 shows the description and specification of $\Re$ parameters. Thus, total shot noise power due to a single LED after using (15) and (8) becomes

$$\left\langle i_{\text{shot}}^2 \right\rangle = 2eB\Re \frac{P_{sr} w}{N}. \tag{16}$$

It is assumed that the required information is recoverable from the nonoverlapping D_n chip only, which is directly detected by the receiving photodiode as in normal intensity modulation. Thus, PIIN noise power is set equal to zero due to the large difference between the auto- and cross-correlation property amongst the intended subscriber and interferer's [4, 7, 23].

Consequently, the total SNR, based on (7), (8), and (16) when the probability of each user transmitting bit 1 at any instant is 1/2, can be written as

$$\text{SNR} = \frac{\left[\Re P_{sr} w / N\right]^2}{eB\Re P_{sr} w / N + 4K_b T_n B / R_L}. \tag{17}$$

The estimated BER, while using Gaussian approximation, for the proposed tree-based hybrid SAC-OCDMA system can be calculated as BER $= (1/2)\text{erfc}\sqrt{\text{SNR}/8}$. Figure 5 shows transmission capacity of the proposed system by varying number of subscribers at performance parameters in Table 1. It is shown that the proposed system provides efficient performance in terms of SNR and BER as we increase the number of subscribers. Fixed cross-correlation property of EMD code reduces interference from adjacent subscribers [8, 15]. Moreover, SDD technique receives the nonoverlapping spectral chip only, which results in maximum difference between auto- and cross-correlation functions at the receiving photodiode [4, 7]. Therefore, SNR and related BER are optimized since both MAI and associated PIIN are eliminated before the signal is converted to electrical domain.

Figure 6 shows system's capacity at different data rates for multiple subscribers while using system parameters in Table 1

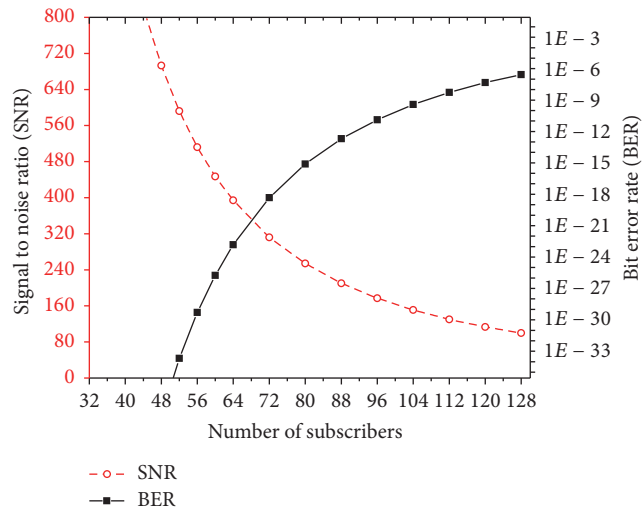

Figure 5: BER and SNR versus number of subscribers at different values of P_{sr}.

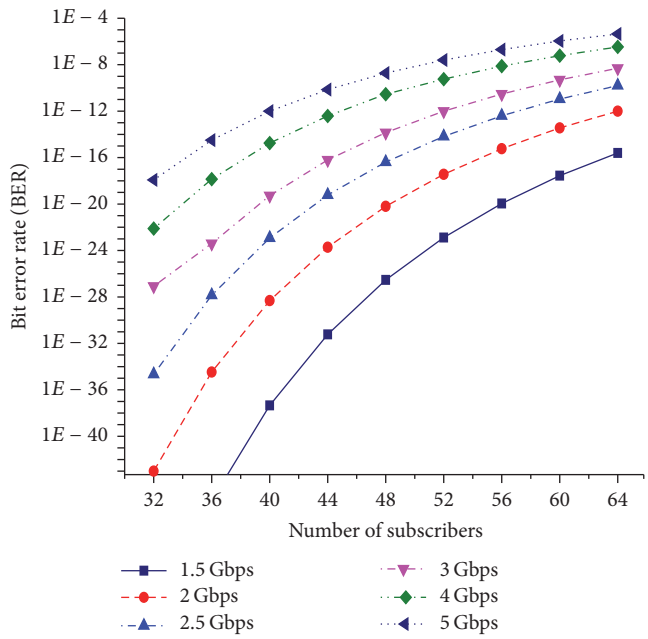

Figure 6: BER versus data rate at different number of subscribers.

[15]. It is shown that quality of received signal deteriorates as we increase the amount of data at the transmitter. Pulse width of the coded signal is inversely proportional to the number of transmitted bits. Therefore, increase in data reduces the pulse width, which makes the system more vulnerable to the effects of dispersion across the medium. However, it is observed that the proposed system is able to handle data rates beyond 2.5 Gbps while maintaining efficient performance parameter, that is, BER of 10^{-9}, owing to its efficient correlation properties in EMD code and recovery of D_n chip only through SDD technique.

Table 2: Simulation parameters.

System parameters	Values
Fiber attenuation	0.25 dB/km
Dispersion	18 ps/nm/km
Fiber length	25 km
PIN responsitivity	0.75 A/W
PIN cutoff frequency	0.75 × Bitrate
P_{sr}	−10 dBm

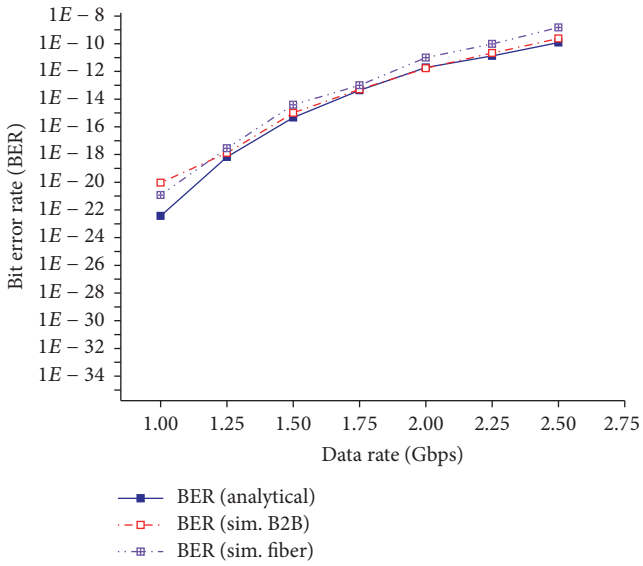

Figure 7: Performance analysis of the proposed tree-based hybrid SAC-OCDMA system.

4.2. Simulation Analysis. OptiSystem is used to analyze transmission capacity of the proposed tree-based hybrid SAC-OCDMA system in comparison with analytic model. Analysis is performed for 64 subscribers, at back-to-back (B2B) and 25 km single mode fiber (SMF) fiber, while using system parameters shown in Table 2. Moreover, EDFA gain and component losses are adjusted to maintain −10 dBm power at the receiving photodiodes. BER and eye pattern are observed at different data rates for performance analysis.

Figure 7 shows transmission capacity of the proposed architecture in comparison with analytic and B2B results. It is observed that simulation and analytic analysis shows proximity with regard to BER for multiple subscribers simultaneously accessing the medium, which validates the performance analysis. Moreover, it is observed that BER increases for B2B, followed by fiber based simulation analysis. It is evident from the fact that fiber introduces dispersion and attenuation to the encoded spectrum, which further deteriorates performance of the system. However, it is not significant enough to disrupt the normal operation. Figure 7 also shows that the use of extra components like switches, OCPs, and so forth for protection has minuscule (almost negligible) effect on performance of the proposed SAC-OCDMA system.

Figure 8 shows eye patterns from the simulation analysis at data rates of 1, 1.5, and 2 Gbps. It is observed that eye opening decreases as the amount of data increases; however, the proposed system is able to provide efficient performance by maintaining nominal eye openings at data rates of up to 2 Gbps.

5. Survivability Analysis

This section outlines the fault detection and restoration capacity of the proposed setup in terms of system initiation, detection, and recovery at both feeder and distribution level.

5.1. Initiation. It is assumed that the proposed system is under normal mode of operation. OLT will start and check the status of FF_p before transmitting any traffic. OLT MAC layer will use discovery gate (DG) packets [13] to check the status of FF_p. If OLT receive acknowledgment (ACK) messages, from all or some ONU modules, for the corresponding DG packets, it will start its transmission using FF_p. However, if no ACK messages are received, OLT will flip the switch towards FF_s and check its status before transmission. OLT will use the same mechanism by sending DG packets to the connected ONUs for the status of FF_s. On the reception of ACK messages from ONUs, OLT will start its operation via FF_s. In case of negative ACKs, OLT will flip the switch towards its original position and wait for a specific time T_s before starting the entire process again.

Similarly, ONUs will check for the connected DFs after initiating their normal operation. They will also send a DG packet towards OLT to check the working status of their corresponding DF. For positive ACK messages, ONU will continue its normal operation through DF. In case of no ACK messages, ONU MAC layer will flip the switch position towards the redundant PF.

While using the same mechanism ONU will check the status of the PF by sending DG packets towards OLT. For positive ACK messages ONU will resume its operation using PF, whereas, in case of negative ACK messages ONU MAC layer will flip the switch towards its initial position and wait for a specific time T_s, before starting the entire process again.

5.2. Feeder Fiber Failure. To understand self-healing mechanism of the proposed protection architecture, it is assumed that system is under normal mode of operation and all traffic, from OLT, is delivered through FF_p. During transmission, OLT will listen to the loss of signal (LOS), which represents the absence of upstream signals from the connected ONUs. In case of no LOS, OLT will continue its normal operation through FF_p with OS_{sa} at port 1.

If failure or cut occurs at point $'f'$ in FF_p as shown in Figure 9, OLT will stop to receive any upstream traffic from the access domain. At the same time, OLT will not be able to transmit any downstream traffic to the connected ONUs, since FF_p is the only transmission medium between OLT and ONUs. This will trigger the LOS flag at OLT.

Consequently, OLT MAC layer will initiate its recovery mechanism and send DG packets towards ONU modules. DG packets will determine the status of FF_p concerning ACK

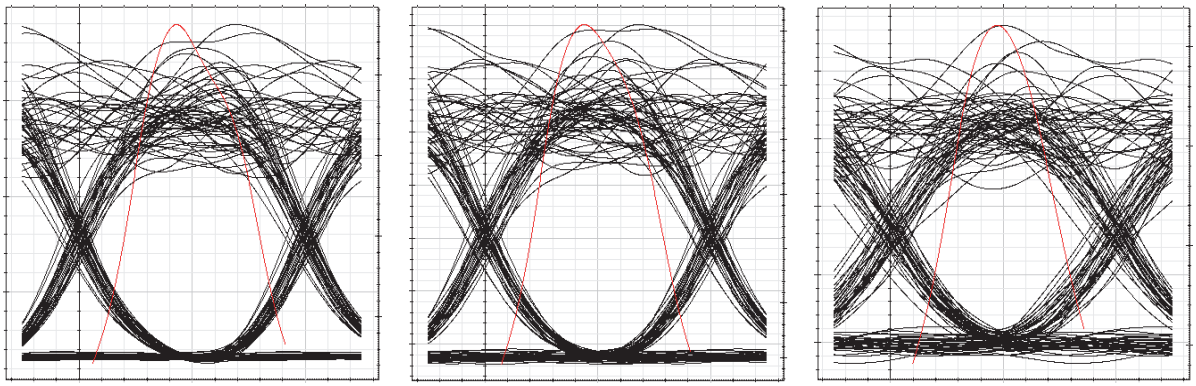

(a) (b) (c)

Figure 8: Eye patterns for the proposed tree-based hybrid SAC-OCDMA system at (a) 1, (b) 1.5, and (c) 2 Gbps of data.

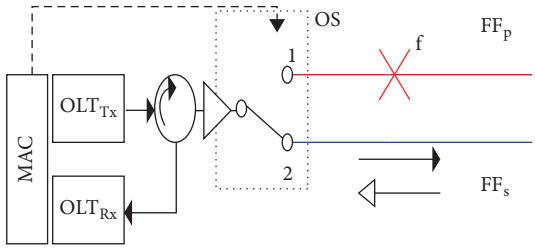

Figure 9: Self-healing mechanism for failure at FF.

messages from ONUs; that is, if OLT receives ACK, from all or some ONUs, for the corresponding DG packets, it will continue its normal operation. However, if no ACK messages are received, OLT will retransmit the DG packets to confirm the fault at the connected FF_p. After several attempts, if no ACK messages are received from the access arena, OLT MAC layer will confirm that FF_p is faulty and flip the switch towards port 2. MAC layer will check the status of FF_s through DG packets, Section 5.1, before transmitting information. For positive ACK messages, MAC layer will direct the OLT to start transmission through the newly switched FF_s as shown in Figure 9.

OLT will continue its normal operation while using FF_s and listen to the LOS until FF_p is repaired. It must be noted that fault at FF will also disconnect the ONUs in access domain. Consequently, they will also initiate their recovery mechanism to resolve the flow of affected traffic, which will lead to unnecessary switching at ONUs. Therefore, it is imperative to increase resolution time and mechanism of fault detection, in ONU modules as compared to OLT. This will avoid the unnecessary switching at ONUs before the issue is resolved at the affected OLT.

5.3. Distribution Fiber Failure. Effect of failure at the DF is not as severe as that of the FF, since the flow of traffic is disrupted to a single ONU. Nevertheless, this needs to be addressed in order to provide high subscriber satisfaction and reduce service interruption penalty costs [11] in case of business subscribers at the access domain. To explain the self-healing mechanism at distribution level of the network, ONU_2 is considered, which is under normal mode of operation. OS_2 is at position 1, and all traffic is sent and received through the corresponding DF. During transmission, ONU_2 will also listen to LOS, which represents the absence of downstream signals from connected OLT. In case of no LOS, ONU_2 will continue its normal operation through its corresponding DF with OS_2 at port 1. In case of failure at point $'c'$ in the DF, ONU_2 will not receive any downstream traffic from OLT. Similarly, OLT will not receive any upstream traffic from ONU_2. This will trigger LOS flag at ONU_2.

Thus, ONU_2 will initiate its recovery mechanism, and MAC layer will send DG packet towards OLT in order to confirm the status of connected DF. On the reception of ACK messages from OLT, ONU_2 will continue its normal operation with OS_2 at position 1. If no ACK message is received from OLT, ONU_2 will perform several attempts to confirm the status of connected DF. The number of DG packets sent by ONU_2 must be twice as that of the ones sent by OLT in order to avoid any unnecessary switching.

For repeated negative ACKs, ONU_2 will confirm the status of failure and flips the switch towards port 2. Consequently, the flow of traffic will shift from DF to the DR between ONU_2 and ONU_3 as shown in Figure 10. Now all traffic from ONU_2 will be sent and received by the DF of ONU_3 through the intermediate PF.

It must be noted that each affected ONU can restore the flow traffic by reconnecting with OLT through its neighboring ONUs, in case of failure at the DF. Based on the same principle, if failure or cut occurs at several DFs, the affected ONUs can share the DFs with working ONUs to reconnect with OLT.

5.4. Restoration Time. The time required for fault detection and restoration can be determined by referring to the autodiscovery process in IEEE 802.3ah [20]. Let T_{dg} represent the time required by OLT to trigger LOS flag and send a DG packet towards the ONU modules. Fault discovery is started after OLT sends the DG packets and takes $2T_{cycle}$ to complete the registration process from a single ONU. In case of negative acknowledgment, OLT will retransmit the DG

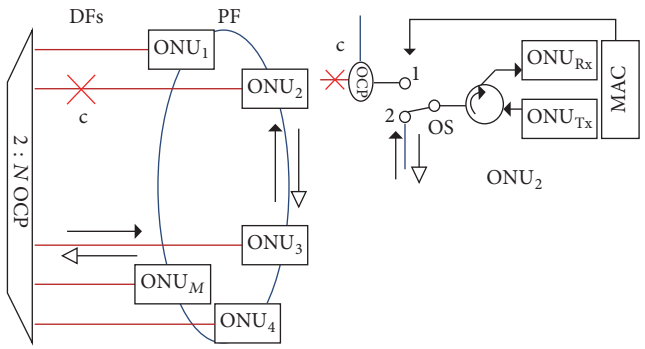

Figure 10: Self-healing mechanism for failure at DF.

packet and wait for $2T_{cycle}$ to receive ACK from at least one ONU module. If no ONU register to the DG packet after two queries, OLT MAC layer will flip the switch position. Consequently, the total time between fault detection and switching operation at feeder fiber failure is $T_{dg} + 2T_{cycle} + 2T_{cycle} + T_{switching}$.

ONU MAC layer adapts the same DG packets for fault detection at the distribution level. Therefore, the time required for fault detection and restoration at ONU modules can be determined through same methodology. However, it is necessary to increase the number of DG packets at ONU modules in order to avoid unnecessary switching for the event of failure at FF_p. Therefore, the time required by ONU MAC layer for fault detection and switching operation is to be given by $T_{dg} + 2T_{cycle} + 2T_{cycle} + 2T_{cycle} + 2T_{cycle} + T_{switching}$.

5.5. Power Budget and Network Capacity. Power budget represents the sum of losses at each component between OLT and ONUs. The purpose of power budgeting in PONs is to ensure the efficient delivery of transmitted data with nominal power ratings, since low power at the PIN photodiode can generate substantial amount of short and thermal noise. Moreover, it also determines the OCP splitting ratio at RN, which translates the number of subscribers in PON. Therefore, it is necessary to analyze power budget of the proposed system in order to ensure high capacity.

For efficient recovery of transmitted information, it is imperative that power received at the PIN photodiode must be greater than its R_{sen}. Table 3 shows the insertion losses at downstream of the proposed tree-based protection architecture for SAC-OCDMA system [14].

If P_{CO} represents the power drop across the central office, which is the sum of insertion losses and gains of optical components at the CO as shown in Table 3, P_{RN} gives the power loss across the FF and $2 : N$ OCP, and P_{DN} is the power loss across the distribution network components, then the downstream power budget P_{DS} can be calculated as

$$\begin{aligned} P_{DS} = {} & P_T - \mathrm{IL}_{OLT} - \mathrm{IL}_{OC_{co}} + P_{EDFA} - \mathrm{IL}_{OS_{co}} - \alpha \mathrm{L}_{FF} \\ & - X\mathrm{IL}_{OCP_{2:NRN}} - \alpha \mathrm{L}_{DF} - \mathrm{IL}_{OCP_{onu}} - \mathrm{IL}_{OS_{onu}} \\ & - \mathrm{IL}_{OC_{onu}} - \mathrm{IL}_{ONU}. \end{aligned} \tag{18}$$

Table 3: Description and specification of network components with power loss.

Description	Parameters	Values
Transmitter power	P_T	0~10 dBm
Insertion loss: OLT	IL_{OLT}	3d Bm
Receiver sensitivity	R_{sen}	−16~−25 dBm
Insertion loss: OS	IL_{os}	0.5 dB
Amplifier gain	P_{EDFA}	25 dB
Insertion loss: OC	IL_{OC}	0.25 dB
Insertion loss: ONU	IL_{ONU}	1 dB
Propagation loss	α	0.25 dB/km
Insertion loss: 1 : 2 OCP	10 log(2)	3 dB

Table 4: Downstream power budget analysis for proposed architecture.

System components	Downstream
BBS power [dBm]	0
CO insertion loss [dB]	3.75
25 Km fiber loss [dB]	6.25
2 : 64 OCP insertion loss [dB]	18
Insertion loss [dB]	4.75
Total losses	−32.75
EDFA gain [dB]	25
Received power [dB]	−7.75
Receiver sensitivity [dBm]	−24

For efficient recovery of transmitted information, it is imperative that

$$P_{DS} \geq R_{sen}. \tag{19}$$

Table 4 shows the downstream power budget for the proposed tree-based hybrid protection architecture, while using insertion losses from Table 4. It is shown that utilization of EDFA at CO can elevate power of the encoded spectrum. Therefore, it can be detected and efficiently recovered at the receiving photodiode. Moreover, without the use of EDFA at the transmitter module, the value of P_{sr} = −10 dBm. This value is significantly lower than required for an error-free recovery. Therefore, a gain of 10 dB and above is required for error-free transmission between OLT and ONU receiver module. Same analogy applies on the upstream traffic, which uses identical encoding and decoding architecture at ONU transmitter and OLT receiver module, respectively.

Furthermore, downstream power budget in Table 4 is determined with 2 : 64 OCP between OLT and ONUs. It is evident that end-face of RN represents the number of ONUs in the access domain. Therefore, the proposed system can easily support 64 subscribers with nominal power ratings at the receiving photodiode. Furthermore, increase in EDFA gain within −5~−30 dB can provide support for desired number of subscribers in the proposed architecture.

Table 5: Components description, connection availability, and cost [11, 12].

System components	Cost ($)	Energy consumption
OLT	12100	20 W, 25 W (with EDFA), 2 W (standby)
ONU	350	1 W, 0.25 W (standby)
Optical circulator	50	
Optical switch	50	
1 : 2, 2 : 2 CPR	50	
1 : N, 2 : N CPR	800	
Fiber (/Km)	160	

6. Cost Analysis

Cost figures of protection architectures are an important parameter, showing the economic benefits for a common end user at the access domain. This section determines overall expenditure of the proposed architecture in comparison with existing ITU-T type C, D, and hybrid architectures while using component costs in Table 5 [11, 24]. Cost figures for PON can be categorized as CAPEX and OPEX [14, 25]. CAPEX represents the investment that is required for the installation and deployment of PON in access domain. CAPEX is calculated by computing the cost of network equipment and fiber infrastructure. Moreover, CAPEX per subscribers is determined by dividing the sum of network equipment and fiber infrastructure costs over the number of subscribers.

OPEX is related to the cost of network operation from the time of deployment till replacement by a new technology. OPEX mainly consists of failure reparation cost, service interruption penalties, and power consumed by active components at OLT and ONUs. Reparation cost depends on the number of failures during the network lifetime. Mean lifetime and MTTR of each component determine the total downtown time per year, which is multiplied by the number of technicians required and their salaries in order to calculate the yearly failure reparation cost. Service interruption penalties include the expenditure that is spent on the fine defined in service level agreement (SLA) between network operators and subscribers. If the service interruption time is higher than a threshold mentioned in SLA, the operator has to pay a fee depending on the interval that the service is unavailable. Power consumption for OPEX is calculated by multiplying the sum of energy consumption of all active components during the network lifetime with the unit price of electrical energy [11, 12, 25, 26].

Analysis is performed for residential customers only and life span of the system is taken as 20 years. Furthermore,

(i) each OLT contains 4 ports with 16 subscribers per port,

(ii) each architecture contains 20 km FF, 5 km DF, and 1 km protection fiber between adjacent ONUs,

(iii) cost of TDM and OCDMA based OLT and ONUs is taken to be the same,

(iv) due to high variation in fiber digging cost, it is assumed that fiber is laid in existing trenches at both feeder and distribution level,

(v) no penalty cost is considered, as only residential customers are considered,

(vi) repairing cost is 1000 $/h,

(vii) per hour cost of electricity is taken to be 0.25 $/kWh.

If M represents the number of PONs and N is the total number of subscribers, then CAPEX equations (base on RBDs) for the considered protection architectures can be written as

$$\begin{aligned}
C_{[C]} &= (M \times \mathrm{OLT} \times \mathrm{OLT}) + (20 \times \mathrm{FF} \times \mathrm{FF}) \\
&\quad + (M \times 2 \times 2 : N\ \mathrm{OCP}) \\
&\quad + (5 \times N \times \mathrm{DF} \times \mathrm{DF}) \\
&\quad + (N \times \mathrm{ONU} \times \mathrm{ONU}) \\
C_{[D]} &= (M \times \mathrm{OLT} \times \mathrm{OLT}) + (20 \times \mathrm{FF} \times \mathrm{FF}) \\
&\quad + (M \times \mathrm{OCP} \times \mathrm{OCP}) \\
&\quad + (M \times 2 \times 2 : N\ \mathrm{OCP}) \\
&\quad + (5 \times N \times \mathrm{DF} \times \mathrm{DF}) \\
&\quad + (N \times \mathrm{ONU} \times \mathrm{ONU}) \\
C_{[H]} &= (M \times \mathrm{OLT} \times \mathrm{OLT}) + (20 \times \mathrm{FR}) \\
&\quad + (M \times \mathrm{OCP}) + (M \times 2 : N\ \mathrm{OCP}) \\
&\quad + (5 \times N \times \mathrm{DF}) + (N \times \mathrm{ONU}) \\
C_{[\mathrm{PT}]} &= (M \times \mathrm{OLT}) + \mathrm{OS} + \mathrm{EDFA} + (20 \times \mathrm{FF} \times \mathrm{FF}) \\
&\quad + (M \times 2 : N\ \mathrm{OCP}) + (5 \times N \times \mathrm{DF}) \\
&\quad + (N \times \mathrm{DR}) + (N \times \mathrm{OCP}) + (N \times \mathrm{OS}) \\
&\quad + (N \times \mathrm{ONU})\,.
\end{aligned} \tag{20}$$

Figure 11(a) shows the deployment cost of different protection architectures. It is observed that the proposed architecture requires minimum CAPEX in comparison with types C, D and hybrid schemes. It is evident from the fact that types C and D duplicate the entire PON, which requires significant

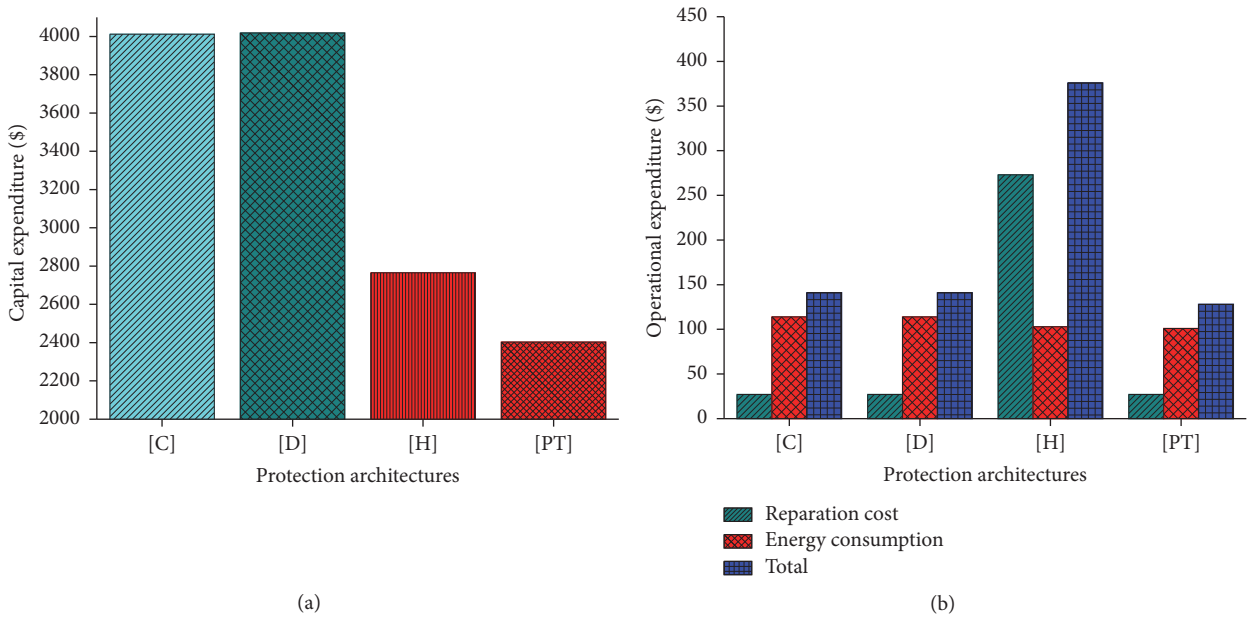

Figure 11: CAPEX and OPEX of existing architectures in comparison with proposed tree-based hybrid SAC-OCDMA system.

amount of CAPEX for deployment. Furthermore, duplication of OLT in hybrid architecture increases the overall cost of deployment as OLT is the most expensive active component in PON, shown in Table 5. Deployment cost of the proposed tree-based protection architecture is relatively low since it avoids duplication of OLT at the CO. Moreover, efficient star-ring redundancy at the distribution level further reduces the cost of deployment by avoiding extensive fiber duplication. As this architecture utilizes minimum components in system construction, therefore energy consumption in Figure 11 is also significantly low.

Figure 11(b) shows expenditure spent on the operation of PONs after deployment. It is observed that hybrid scheme requires the highest OPEX since no protection is provided at the distribution level. This significantly elevates the network downtime per year and more resources are spent on detecting and recovering faults. Figure 11(b) shows that the proposed architecture along with types C and D requires minimum reparation cost, owing to desirable connection availability and minimal downtime per year. Moreover, no duplication at OLT and ONU significantly reduces energy consumption of the proposed architecture as compared to types C, D and hybrid networks.

Consequently, the proposed tree-based hybrid SAC-OCDMA system requires minimum cost of deployment and operation as shown in Figure 12, due to

(i) efficient star-ring topology that reduces the amount of DF and hence the cost required for deployment,

(ii) no redundant OLT and ONU, which reduce the deployment cost and energy consumption over the network life time,

(iii) fault detection and restoration at both feeder and the distribution level, which significantly reduce the network downtime per year. Consequently minimum resources are spent on repairing.

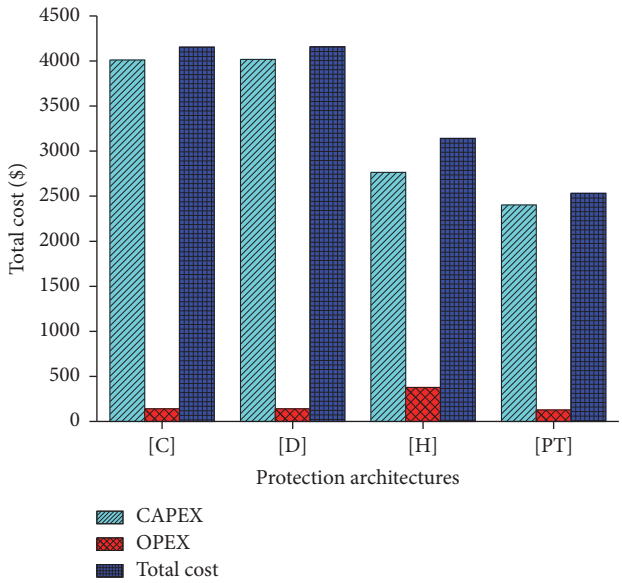

Figure 12: Total cost for different protection architectures.

7. Conclusion

Efficient operation of PON requires a reliable architecture, which is able to provide high network capacity along with fault detection and restoration mechanism. This paper proposes a novel tree-based hybrid SAC-OCDMA system with EMD code and two-tier protection. EMD code significantly elevates performance of the proposed system by negating MAI and PIIN through efficient correlation properties along

with nominal values of N and w. Analysis shows that EMD code along SDD technique enables the proposed system to support high data rates at desirable number of subscribers. Moreover, protection at both feeder and distribution networks ensures ubiquitous transmission of affected traffic from faulty to working fiber. Furthermore, star-ring protection and MAC controlled switching enable the proposed system to provide the necessary protection at minimum power loss, CAPEX, and OPEX. Thus, the proposed tree-based hybrid SAC-OCDMA system is highly suitable for future PONs owing to its significant advantages like support for high capacity in terms of data and the number of subscribers, ease of implementation, relatively simple architecture, immediate fault detection and restoration at both feeder and distribution networks, and minimum cost as compared with existing solutions.

Conflicts of Interest

The authors declare that they have no conflicts of interest.

References

[1] E. Wong, "Next-generation broadband access networks and technologies," *Journal of Lightwave Technology*, vol. 30, no. 4, Article ID 6094146, pp. 597–608, 2012.

[2] X. Wang, N. Wada, T. Miyazaki, G. Cincotti, and K.-I. Kitayama, "Hybrid WDM/OCDMA for next generation access network," in *Asia-Pacific Optical Communications*, pp. 678328-678328, nternational Society for Optics and Photonics, 2007.

[3] H. Yin and D. J. Richardson, "Optical code division multiple access communication networks," *chap*, vol. 1, pp. 36-37, 2008.

[4] H. Ghafouri-Shiraz and M. M. Karbassian, *Optical CDMA Networks: Principles, Analysis and Applications*, John Wiley & Sons, 2012.

[5] N. Din Keraf, S. A. Aljunid, A. R. Arief, and P. Ehkan, "The evolution of double weight codes family in spectral amplitude coding ocdma," *Advanced Computer and Communication Engineering Technology*, pp. 129–140, 2015, Springer.

[6] F. Su and H. Jin, "Research of code construction for ocdma system," in *Advances in Mechanical and Electronic Engineering*, pp. 265–270, Springer, 2013.

[7] T. H. Abd, S. A. Aljunid, H. A. Fadhil, R. A. Ahmad, and N. M. Saad, "Development of a new code family based on SAC-OCDMA system with large cardinality for OCDMA network," *Optical Fiber Technology*, vol. 17, no. 4, pp. 273–280, 2011.

[8] H. A. Fadhil, S. A. Aljunid, and R. B. Ahmad, "Performance of random diagonal code for OCDMA systems using new spectral direct detection technique," *Optical Fiber Technology*, vol. 15, no. 3, pp. 283–289, 2009.

[9] H. Y. Ahmed and K. S. Nisar, "Diagonal Eigenvalue Unity (DEU) code for spectral amplitude coding-optical code division multiple access," *Optical Fiber Technology*, vol. 19, no. 4, pp. 335–347, 2013.

[10] M. H. Kakaee, S. Seyedzadeh, H. Adnan Fadhil, S. Barirah Ahmad Anas, and M. Mokhtar, "Development of Multi-Service (MS) for SAC-OCDMA systems," *Optics and Laser Technology*, vol. 60, pp. 49–55, 2014.

[11] L. Wosinska, J. Chen, and C. P. Larsen, "Fiber access networks: Reliability analysis and Swedish broadband market," *IEICE Transactions on Communications*, vol. E92-B, no. 10, pp. 3006–3014, 2009.

[12] K. Grobe, M. Roppelt, A. Autenrieth, J.-P. Elbers, and M. Eiselt, "Cost and energy consumption analysis of advanced WDM-PONs," *IEEE Communications Magazine*, vol. 49, no. 2, pp. S25–S32, 2011.

[13] W. A. Imtiaz, Y. Khan, and K. Mahmood, "Design and analysis of self-healing dual-ring spectral amplitude coding optical code division multiple access system," *Arabian Journal for Science and Engineering*, vol. 41, no. 9, pp. 3441–3449, 2016.

[14] A. Waqas, *Design and feasibility of optical code division multiple access system for fiber-to-the-home networks [Ph.D. Dissertation]*, 2016.

[15] W. A. Imtiaz, M. Ilyas, and Y. Khan, "Performance optimization of spectral amplitude coding OCDMA system using new enhanced multi diagonal code," *Infrared Physics and Technology*, vol. 79, pp. 36–44, 2016.

[16] M. Kavehrad and D. Zaccarin, "Optical Code-Division-Multiplexed Systems Based on Spectral Encoding of Noncoherent Sources," *Journal of Lightwave Technology*, vol. 13, no. 3, pp. 534–545, 1995.

[17] S. Ayotte and L. A. Rusch, "Increasing the capacity of SAC-OCDMA: Forward error correction or coherent sources?" *IEEE Journal on Selected Topics in Quantum Electronics*, vol. 13, no. 5, pp. 1422–1428, 2007.

[18] K.-I. Kitayama, X. Wang, and N. Wada, "OCDMA over WDM PON - Solution path to gigabit-symmetric FTTH," *Journal of Lightwave Technology*, vol. 24, no. 4, pp. 1654–1662, 2006.

[19] S. S. Pawar and R. K. Shevgaonkar, "Modelling of FBG for encoding/decoding in SAC-OCDMA system," in *Proceedings of the International Conference on Next Generation Networks*, pp. 1–4, ind, September 2010.

[20] B. T. Lee, M. S. Lee, and H. Y. Song, "Simple ring-type passive optical network with two-fiber protection scheme and performance analysis," *Optical Engineering*, vol. 46, no. 6, Article ID 065002, 2007.

[21] P. Lafata and J. Vodrazka, "Simulation of ring-based passive optical network and its experimental verification," *Elektronika ir Elektrotechnika*, vol. 19, no. 5, pp. 93–98, 2013.

[22] C.-H. Yeh and S. Chi, "Self-healing ring-based time-sharing passive optical networks," *IEEE Photonics Technology Letters*, vol. 19, no. 15, pp. 1139–1141, 2007.

[23] S. Mostafa, A. E.-N. A. Mohamed, F. E. Abd El-Samie, and A. N. Z. Rashed, "Performance Analysis of Diagonal Eigenvalue Unity (DEU) Code Using NAND Subtraction and Spectral Direct Detection Techniques and Its Use with Triple-Play-Services in SAC-OCDMA," *Wireless Personal Communications*, vol. 85, no. 4, pp. 1831–1849, 2015.

[24] X. Zhao, X. Chen, and X. Fu, "A novel protection switching scheme for pons with ring plus tree topology," in *Asia-Pacific Optical Communications*, pp. 60223H–60223H, International Society for Optics and Photonics, 2005.

[25] M. Mahloo, "Reliability versus Cost in Next Generation Optical Access Networks [Ph.D. thesis]," Tech. Rep., KTH Royal Institute of Technology, 2013.

[26] J. Chen and L. Wosinska, "Analysis of protection schemes in PON compatible with smooth migration from TDM-PON to hybrid WDM/TDM-PON," *Journal of Optical Networking*, vol. 6, no. 5, pp. 514–526, 2007.